The electronic properties of Si(001)–Bi(2 × *n*)

2005 J. Phys.: Condens. Matter 17 571

(http://iopscience.iop.org/0953-8984/17/4/001)

INSTITUTE OF PHYSICS PUBLISHING JOURNAL OF PHYSICS: CONDENSED MATTER

J. Phys.: Condens. Matter **17** (2005) 571–580 doi:10.1088/0953-8984/17/4/001

The electronic properties of Si(001)–Bi(2 × n)

A G Mark[1], J A Lipton-Duffin[1], J M MacLeod[1], R H Miwa[2], G P Srivastava[3] and A B McLean[1]

[1] Department of Physics, Queen's University, Kingston, ON, K7L 3N6, Canada
[2] Faculdade de Física, Universidade Federal de Uberlândia, CP 593, 38400-902, Uberlândia, MG, Brazil
[3] School of Physics, University of Exeter, Stocker Road, Exeter EX4 4QL, UK

E-mail: mclean@physics.queensu.ca

Received 2 October 2004, in final form 29 November 2004
Published 14 January 2005
Online at stacks.iop.org/JPhysCM/17/571

Abstract

A Bi $2 \times n$ surface net was grown on the Si(001) surface and studied with inverse photoemission, scanning tunnelling microscopy and *ab initio* and empirical pseudopotential calculations. The experiments demonstrated that Bi adsorption eliminates the dimer related π_1^* and π_2^* surface states, produced by correlated dimer buckling, leaving the bulk bandgap clear of unoccupied surface states. *Ab initio* calculations support this observation and demonstrate that the surface states derived from the formation of symmetric Bi dimers do not penetrate the fundamental bandgap of bulk Si. Since symmetric Bi dimers are an important structural component of the recently discovered Bi nanolines, that self-organize on Si(001) above the Bi desorption temperature, a connection will be made between our findings and the electronic structure of the nanolines.

1. Introduction

The Si(001)/Bi monolayer system (figure 1) is important because Bi can be used as a strain-relaxing surfactant in Si/Ge hetero-epitaxy (Sakamoto *et al* 1993). Below the Bi desorption temperature of $T_d \approx 500\,^{\circ}$C, Bi forms a $2 \times n$ surface net on Si(001) (Appelbaum *et al* 1976, Rohlfing *et al* 1995, Gay *et al* 1998a, 1998b, Asahi *et al* 2000). Whereas the $2\times$ periodicity is caused by Bi dimer formation, the $n\times$ periodicity is caused by the formation of ordered rows of Bi dimer vacancies (Naitoh *et al* 1997, Park *et al* 1994, Bowler and Owen 2002). The vacancy rows relax overlayer strain and the value of n lies in the range 5–12, depending on both the Bi coverage and the annealing temperature (Park *et al* 1994). The formation of the dimer vacancies is expected because the covalent radii of Bi (1.46 Å) and Si (1.17 Å) are very dissimilar.

In this paper we report the results of an investigation of the $2 \times n$ phase using inverse photoemission, scanning tunnelling microscopy (STM) and *ab initio* and empirical pseudopotential calculations. Interestingly, recent studies of Bi growth on Si(001) surfaces

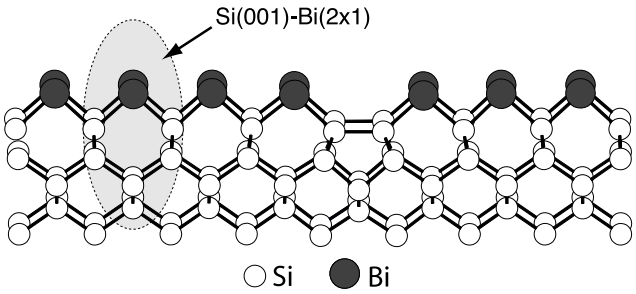

Figure 1. A side view of a Bi overlayer on Si(001). The $\times 2$ order is due to Bi dimers and the $\times n$ order is due to missing Bi dimers.

above T_d have discovered a self-organized nanoline motif with an exceptionally high degree of structural order (Naitoh *et al* 1997, 1999, Miki *et al* 1999b, 1999a, Naitoh *et al* 2000, 2001, Bowler and Owen 2002, Owen *et al* 2002b, 2002a, 2003). These lines can be grown to lengths of up to 500 nm without breaks or kinks (Miki *et al* 1999a, Owen *et al* 2003) and the growth of the lines is thought to involve the reconstruction of up to three silicon layers (Owen *et al* 2002b). The aim of the present study is to provide a more complete understanding of the geometric and electronic structure of the $2 \times n$ phase. The $2 \times n$ overlayer phase is structurally simpler than the nanoline phase. In particular, we wanted to experimentally confirm the presence of the symmetric Bi dimers in the $2 \times n$ phase because it is thought that the $2 \times n$ phase and the nanolines share the symmetric Bi dimer as a common motif.

2. Experimental and theoretical details

The experimental studies were performed with an inverse photoemission system (Lipton-Duffin 2001, Lipton-Duffin *et al* 2002, 2004) and also a beetle-type STM (MacLeod *et al* 2003) using a Pt–Ir tip that was sharpened by field emission. The inverse photoemission system has a Stoffel–Johnson electron source (Stoffel and Johnson 1984) and two Geiger–Müller photon detectors (Johnson and Hulbert 1990) that are run concurrently to maximize the solid angle of detection. Ethanol was used as a self-quenching detection gas in the photon detectors (Lipton-Duffin *et al* 2002) and gating electronics were used to correct for the finite detector dead-time ($\approx$150 μs) (Lipton-Duffin *et al* 2002). The detectors have a mean detection energy of $\hbar\omega_d = (10.61 \pm 0.07)$ eV and a bandpass of $\Delta\hbar\omega_d = (0.35 \pm 0.05)$ eV.

N-type Si(001) wafers, with resistivities in the range of 5.2–7.2 Ω cm (Virginia Semiconductor, Inc.), were diced into rectangular samples with a width of 6 mm and a length of 17 mm. Following an overnight degas, atomically ordered surfaces were prepared by resistively heating the samples to 1260 °C for 40 s while maintaining the chamber pressure below 5×10^{-10} Torr, annealing at 1000 °C for 180 s, and then cooling the sample at a rate of $\approx$1 °C s^{-1}. This procedure yielded sharp two-domain Si(001)(2×1) low energy electron diffraction (LEED) patterns, with a low background. High purity Bi was evaporated from a quartz crucible at rates that lay in the range 0.1–0.3 Å min^{-1}. During deposition the substrate was raised to a maximum temperature of 400 °C and after deposition the overlayers were annealed at this temperature for up to 15 min. Diffraction patterns had superlattice spots consistent with the formation of a double-domain $2 \times n$ overlayer. Attempts were made to grow single-domain Si(001)–Bi(2×1) overlayers on vicinal Si(001) surfaces (Cricenti *et al* 1993). However, our studies did not provide surfaces with clear single-domain structure and consequently we did not perform momentum-resolved studies off-normal.

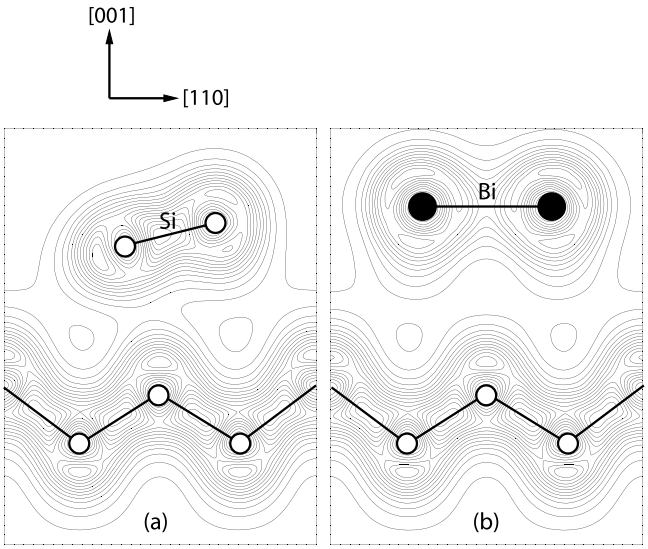

Figure 2. (a) Schematic, side view, structural models of the Si(001)(2 × 1) surface with asymmetric Si dimers and (b) the Si(001)–Bi(2 × 1) surface with symmetric Bi dimers and calculated total charge densities. The white spheres represent Si atoms and the black spheres represent Bi atoms. On flat Si(001) surfaces there are two equally populated 2 × 1 domains rotated by $\pi/2$ w.r.t. one another. Correlated dimer buckling produces locally a c(4 × 2) surface net.

Theoretical calculations were made by considering a full monolayer of Bi, forming the Si(001)–Bi(2 × 1) structure, shown in figure 2, characterized by the breaking of Si dimers and the formation of Bi dimers along the original Si dimer rows. The non-local pseudopotential method, together with the local density approximation (LDA), was applied to an artificially repeated supercell geometry. A plane wave basis set, up to a 12 Ryd kinetic energy cut-off, was used. This is 4 Ryd higher than used previously (Gay *et al* 1998a), allowing us to expand the basis set. Details of the method, the atomic geometry and some previously published theoretical results for this system can be found elsewhere (Srivastava 1999, Gay *et al* 1998a). We have not performed quasi-particle calculations in this study because we are primarily interested in the changes in the surface electronic structure that are induced by Bi adsorption. It has previously been shown that the major difference between quasi-particle bands and the LDA bands is that the unoccupied quasi-particle bands are rigidly shifted to higher energy. Consequently, a direct comparison of the Si(001)(2 × 1) and the Si(001)–Bi(2 × 1) DOS calculated using the LDA is sufficient for our purposes.

3. Results

A constant current STM topograph collected from a Bi covered Si(001) surface that displayed clear $2 \times n$ order with $n = 6 \pm 0.8$ and some second monolayer Bi growth is shown in figure 3. The surface contains two $2 \times n$ domains that are separated by a single height step and related by a rotation of $\pi/2$. Areas of the surface that have dimer rows running approximately vertical have been labelled v and areas for the surface that have dimer rows running approximately horizontal have been labelled h. The presence of two surface phases is expected because Si has the diamond crystal structure and a single height step ($\frac{1}{4}a_\circ$ where $a_\circ$ is the cubic lattice constant) rotates the tetrahedral bonding directions by $\pi/2$. In the STM image, the Bi dimers

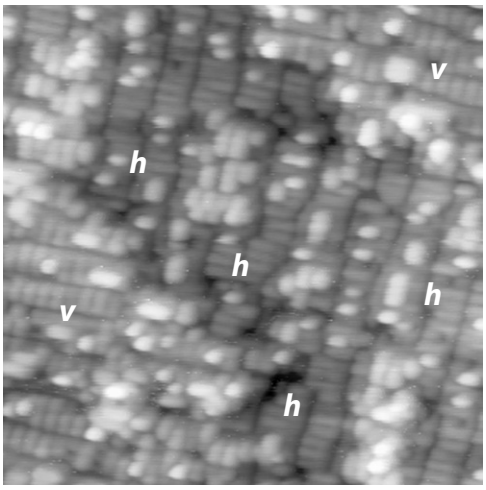

Figure 3. STM constant current topograph of the double-domain Si(001)–Bi($2 \times n$) surface. Regions of the surface that have Bi-dimer rows running approximately vertical are labelled v and regions that have Bi-dimer rows running approximately horizontal are labelled h. Areas labelled v are separated by a single height step from areas labelled h. The step rotates the dimerization direction by $\pi/2$. In this image there is some second layer Bi growth (bright spots). Image area $= (30\ \text{nm})^2$. Image bias $= -1.50$ V (full states).

within the rows appear to be symmetric. There are, for example, no pinned zig-zag dimer rows near surface defects that are frequently found on Si(001) surfaces. On Si(001) the π-like surface bands for a symmetric dimer configuration are half full and the surface can lower its energy by allowing the dimers in the surface layer to asymmetrically tilt. Although the geometric structures of the Si(001) and the Si(001)–Bi(2×1) systems are similar, the fact that Bi has one extra valence electron means the π-like surface bands are full and tilting the Bi dimers does not produce the same energy gain.

The image reproduced in figure 3 was taken with negative sample bias (full states). We found that the surface was difficult to image with positive sample bias (empty states). This observation is consistent with the results of the inverse photoemission study to be described below. In this particular case, 1.5 ML of Bi was deposited over 13 min onto a Si(001) surface that was maintained at a temperature of 590 °C. The surface was not post-annealed and regions of the surface, as might be expected from the temperature during deposition, also contained Bi nanolines (not shown). However, this part of the surface displays $2 \times n$ order with some additional second layer Bi growth.

In figure 4(a) an isochromat inverse photoemission spectrum collected at the centre of the surface zone ($\overline{\Gamma}$) from the two-domain Si(001)(2×1) surface is presented together with a spectrum that was collected at $\overline{\Gamma}$ from an ordered Si(001)–Bi($2 \times n$) overlayer (figure 4(b)). The lower spectrum has been shifted by 0.35 eV, to line up the feature marked β and, to first order, 0.35 eV is the Bi-induced band bending shift. The sign and magnitude of the band bending shift is in good agreement with the results of recent core-level photoemission studies of Bi adsorption on Si(001) using synchrotron radiation (Corradini *et al* 1999). The π_1^* and π_2^* surface states were probed at $k_\parallel = 0$ ($\overline{\Gamma}$). Although only one unoccupied state is expected on the 2×1 surface, two states are observed with inverse photoemission (Cricenti *et al* 1995, Johansson and Reihl 1992). This is consistent with the presence (Cricenti *et al* 1995, Johansson and Reihl 1992) of correlated dimer buckling at room temperature (Wolkow 1992, Northrup

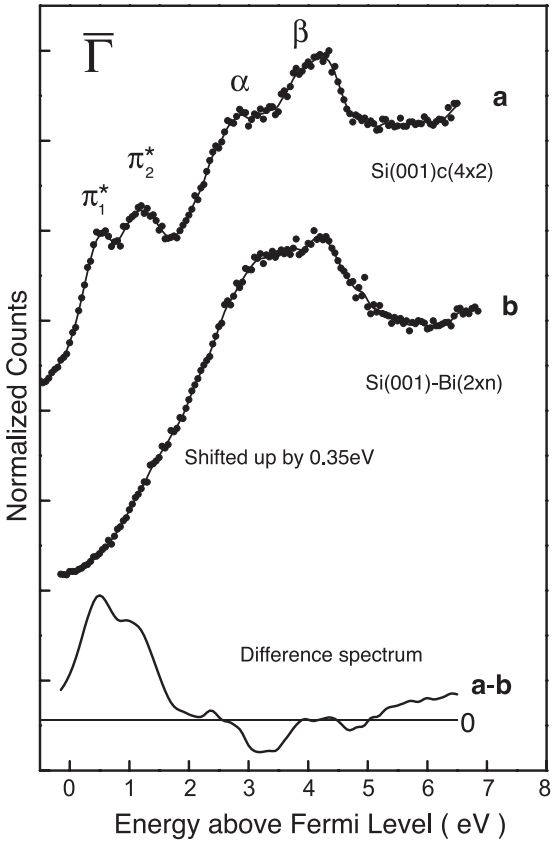

Figure 4. Inverse photoemission spectra collected at $\overline{\Gamma}$ of (a) the Si(001) surface showing the π_1^* and the π_2^* unoccupied surface states and (b) the Si(001)–Bi(2 × *n*) epitaxial monolayer system. The curve in the lower portion of the figure is a difference spectrum, generated by normalizing spectrum (b) to (a) at β and subtracting (b) from (a).

1993, Cricenti *et al* 1995, Johansson and Reihl 1992). The two occupied, π_1 and π_2, and the two unoccupied, π_1^* and π_2^*, bands of surface states are derived from the four dangling bonds of the Si(001)-c(4 × 2) surface net (Northrup 1993) and figure 4(a) demonstrates that c(4 × 2) order is still present at room temperature. Fourteen n-type surfaces were studied and estimates for the state positions were obtained by averaging the results from all surfaces. The $\pi_1^* - E_F$ splitting, where E_F is the Fermi level, was found to be (0.51 ± 0.1) eV. This value is larger than previous inverse photoemission estimates (Cricenti *et al* 1995, Johansson and Reihl 1992) that placed π_1^* closer to the Fermi level (0.35–0.4 eV). However, our lowest estimates for this splitting do lie in this range. Furthermore, we resolved the π_2^* state at $\overline{\Gamma}$ on all samples, consistent with the predictions of *ab initio* calculation (Northrup 1993). The π_2^* state was also present on single-domain vicinal Si(001) surfaces (4°) that we studied that are not included in the above averages. The π_2^* band does overlap the conduction band continuum at $\overline{\Gamma}$ and so it is possible (see later) for the π_2^* surface state band to be obscured by the conduction band states. Our estimate of the $\pi_2^* - \pi_1^*$ splitting (0.73 ± 0.08) eV is in excellent agreement with the value obtained previously using inverse photoemission (0.75 eV), averaging over the $\overline{\Gamma J}$ direction (Johansson and Reihl 1992), and slightly lower than a value determined recently in a two-photon photoemission study (0.82 eV) (Kentsch *et al* 2002).

In contrast to the results presented here, we note that previous inverse photoemission studies of single-domain Si(001)(2 × 1) surfaces (Cricenti *et al* 1995, Johansson and Reihl 1992) did not resolve π_2^* at $\overline{\Gamma}$. To resolve the state, they had to go into the second surface Brillouin zone to $\overline{\Gamma_2}$. The most natural explanation for this difference is that the overlap with the conduction band continuum (Northrup 1993) obscured π_2^* at $\overline{\Gamma}$ in the earlier experiment. The experimental geometries and also the detection energies in the two experiments are different. Consequently, it is unsurprising that the experimental spectra are not identical.

The curve in the lower portion of figure 4 is a difference spectrum, generated by subtracting (b) from (a). This curve clearly illustrates that the growth of the overlayer eliminates both of the unoccupied surface states without producing intense new adsorbate-induced unoccupied states at $\overline{\Gamma}$. We note that although relatively few studies of epitaxial growth on Si(001) have been performed with inverse photoemission (Reihl *et al* 1989, P and B 1989, Himpsel 1990b, Himpsel 1990a, Cricenti *et al* 1993 n.d.[4]), studies of epitaxial overlayer growth on Si(111) (e.g. Cu (Reihl *et al* 1989), Ag (Reihl *et al* 1989), Au (Reihl *et al* 1989), B (Himpsel 1990b, 1990a), Al (Reihl *et al* 1989), Ga (Reihl *et al* 1989), In (Reihl *et al* 1989, Himpsel 1990a) and Ge (Reihl *et al* 1989, P and B 1989)) find clear adsorbate-induced levels between the Fermi level and the vacuum level, the exception to this rule being elements from group V (e.g. As (Himpsel 1990b, 1990a)) that act as dopants in bulk Si and fill the unsaturated dangling bond on Si(111), producing an occupied lone pair state. Bismuth acts in a similar fashion on Si(001).

For the full monolayer coverage of Bi, the Si dimer is broken and Bi dimers are formed along the original Si dimer rows. Theoretical considerations lead us to believe that the Bi dimers are symmetric, leading to the formation of the Si(001)–Bi(2×1) structure. Experimental evidence for symmetric dimers, or more accurately the lack of asymmetric dimers, can be found from figure 3, published STM images (Hanada and Kawai 1990, 1991, Park *et al* 1993, 1994) and the fact that the Bi 5d core level is found to have only one spin–orbit split component up to Bi coverages of one monolayer (Corradini *et al* 1999). Asymmetric dimers would produce two spin–orbit split components because there would be two inequivalent surface sites. The Si dimer related states π_2, π_1^* and π_2^* are replaced by the Bi dimer related π, π^* and ppσ^* states, as shown in figure 5 and also figures 10(b)–(d) in Gay *et al* (1998a). As mentioned above, due to the availability of a sufficient number of electrons from the Bi atoms, the π and π^* states are occupied and lie inside the bulk valence band region. The application of the local density approximation indicates that the ppσ^* state lies close to the conduction band edge. (It is well known that the energies of unoccupied states are generally pushed upwards when a proper quasi-particle calculation is performed. Such an upward shift of unoccupied states is usually more pronounced for surface states than bulk states (Srivastava 1999).) The density-of-states calculations (figure 5) were performed using 12 special k-points distributed throughout the surface Brillouin zone and by including all states in the supercell. Although only the region around the zone centre is probed in the inverse photoemission spectrum (± 0.05 Å^{-1}) we have calculated the DOS averaged over the entire surface Brillouin zone because the surface bands have a fairly shallow dispersion. However, a detailed comparison of experiment and theory requires the surface energy bands (Gay *et al* 1998a). From these we infer that the ppσ^* band overlaps the bulk continuum at the zone centre. The experimental curve obtained from the Si(001)–Bi(2 × n) system (figure 4) does contain a weak shoulder 1.5 eV above the Fermi level that could be the ppσ^* band obscured by the bulk transition. From the calculated surface energy bands we also infer that the ppσ^* band splits off from the bulk continuum as it approaches the surface Brillouin zone boundary ($\overline{J}$). Consequently, $\overline{J}$ would be the most

[4] The inverse photoemission cross-section of Si(001) is approximately a factor of three times smaller than that of Si(111) at the electron and detector energies used in this study.

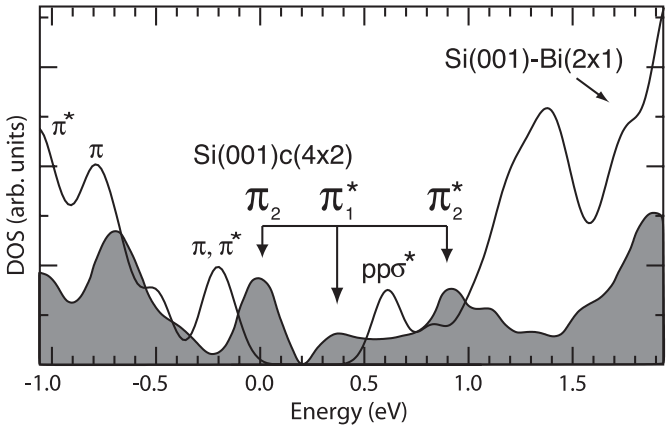

Figure 5. Calculated density of states (DOS) for Si(001) (shaded) and the Si(001)–Bi(2 × 1) epitaxial overlayer system. All surface and bulk states in the surface Brillouin zone are included. The energy zero is the Si valence band maximum. The growth of the Bi overlayers eliminates the π_2, π_1^* and π_2^* states. They are replaced by π, π^* and ppσ^* states associated with the symmetric Bi dimer structure in the epitaxial overlayer. Although the ppσ^* band overlaps the bulk continuum at the zone centre, it splits off from the bulk energy bands as it approaches the surface Brillouin zone boundary ($\overline{J}$). Due to the state's strict localization on the surface plane, the cross-section for an inverse photoemission transition into this state may be weak.

natural place to probe this state if it were possible to grow single-domain Si(001)–Bi(2 × 1) overlayers.

An assumption that has been made in these calculations is that the electronic structure of the Si(001)–Bi(2 × 1) system is representative of the electronic structure of the Si(001)–Bi(2 × *n*) system. Another way of stating this is that we have assumed that the rows of missing Bi dimers that appear in the Bi overlayer do not have an appreciable effect on the electronic structure. This seems reasonable based on our theoretical and experimental studies of the GaAs(110)–Bi(1 × 1) system (McLean and Himpsel 1989, McLean *et al* 1991). This system contains discommensurate misfit dislocations that are not dissimilar to the Bi dimer vacancy rows. We found that rows of Bi vacancies in the Bi(1 × 1) structure on GaAs(110) produced no noticeable effect on the surface electronic structure of the system; the surface bands were measured using angle-resolved photoemission and compared with the calculated surface bands. However, we are currently testing this assumption using a larger surface unit cell and explicitly including the vacancy dimer rows. The results of this study will be reported in a future publication.

The large peaks located at 2.86 and 4.14 eV above the Fermi level, that dominate both inverse photoemission spectra, have previously been attributed to transitions between unoccupied bulk energy bands of Si (Johansson and Reihl 1992, Ortega and Himpsel 1993). To identify the energy bands involved in the transitions, the band structure of Si was calculated along the Γ–X and the $\frac{2}{3}\Sigma$–L lines (figures 6 and 7). The conduction band results presented in figure 7 were obtained by employing the empirical pseudopotential method, using the atomic form factors presented in Chelikowsky *et al* (1989). The valence and conduction band results obtained from this method are in agreement with optical transition measurements, and thus the higher conduction bands are the best predictions available. The latter peak can be reached by a surface umklapp process involving the $\vec{g}(\frac{1}{2}, 0)$ vector (or equivalently, the $\vec{g}(0, \frac{1}{2})$ vector in the rotated domain). This reciprocal lattice vector is associated with the 2×, dimerization-induced, translational symmetry of the (2 × 1) overlayer. All possible transitions along these

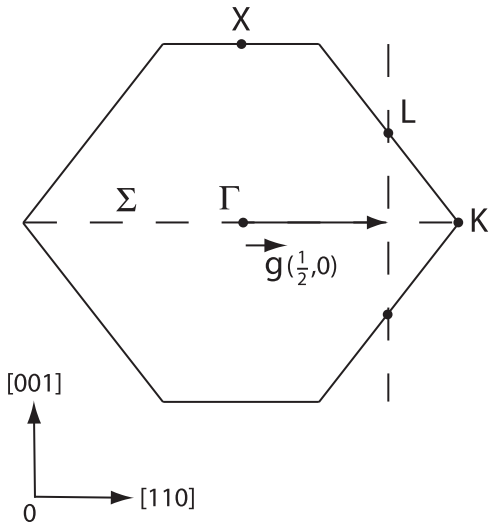

Figure 6. Side view of the Si bulk Brillouin zone. When the incoming electrons are antiparallel to the (001) surface normal, the bulk transitions are located along the Γ–X line. The dashed line, two-thirds of the way from Γ to K along the Σ high symmetry line, can also be accessed by a surface umklapp process involving the $\vec{g}(\frac{1}{2}, 0)$ vector.

two lines, involving a photon equal to our isochromat detection energy ($\hbar\omega_d = 10.61$ eV), were calculated from the bulk bandstructure, and the two transitions that match the experimental initial energies are shown in figure 7. Previously, a similar approach was used to analyse normal incidence inverse photoemission spectra collected in the initial energy range, measured relative to the vacuum level, from 14.5 to 21.5 eV (Ortega and Himpsel 1993). These authors also identified a radiative transition from the primary cone to the Δ_2' band. This is the transition labelled α in figure 7. It is interesting to note that the shape of the spectrum, in the energy range that contains the two bulk transitions, changes when Bi is adsorbed; the transition that has been labelled β loses intensity relative to the α transition. Although this could be due to a suppression of surface related features, that are not resolved in the spectrum, it is also possible that the formation of the ordered Bi overlayer affects the two transitions differently, because one involves a surface umklapp process. Although the latter possibility is intriguing, it is impossible for us to differentiate between these two scenarios in the experiment.

4. Conclusions

We have studied the Si(001)–Bi($2 \times n$) monolayer system using inverse photoemission, STM and a combination of *ab initio* and empirical pseudopotential calculations. The experimental spectra collected from the Si(001) system have four peaks that can be clearly resolved with inverse photoemission. They have been labelled π_1^*, π_2^*, α and β. For the Si(001)–Bi system, the two most intense peaks (α and β), although translated by the band bending shift, remain largely unaltered by Bi deposition. Based on the calculated band structure results, the peaks α and β are identified as Si bulk transitions, in excellent agreement with our inverse photoemission results and previous experimental studies of the Si bulk bandstructure using inverse photoemission (Ortega and Himpsel 1993). Our calculations demonstrate that the unoccupied π_1^* and π_2^* surface state bands on Si(001) are replaced by the π and π^* surface state bands associated with the symmetric Bi-dimer structure. The latter lie below the valence

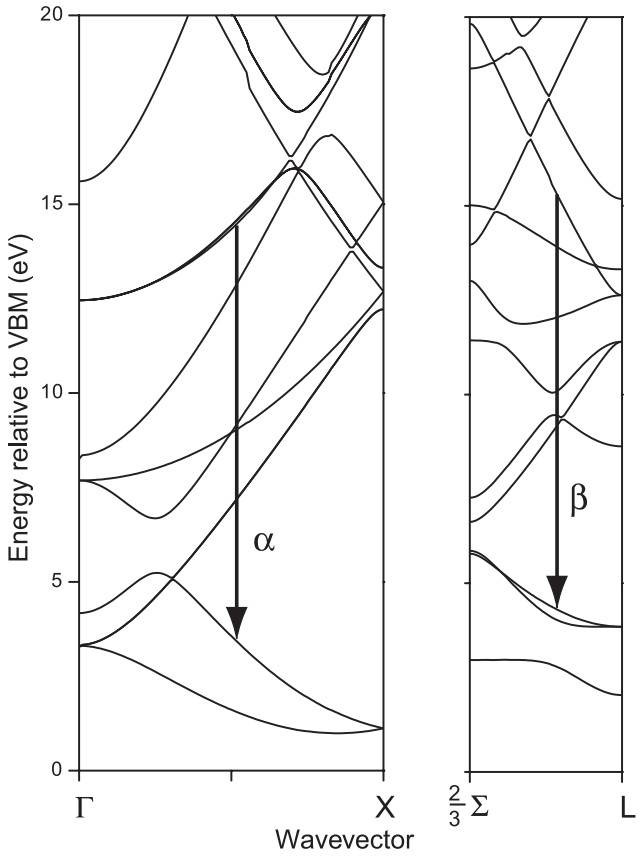

Figure 7. In the left panel, the bulk Si energy bands along Γ–X are shown together with a possible transition involving a photon with an energy equal to our detection energy; $\hbar\omega_{\mathrm{d}} = 10.61$ eV. Surface umklapp scattering via $\vec{g}(\frac{1}{2}, 0)$ also makes the $\frac{2}{3}\Sigma$–L line accessible (right panel). The α and β transitions were selected from the many possible transitions that conserve energy by matching the initial energies to the experimental values.

band maximum and are therefore invisible to inverse photoemission. The lack of unoccupied states close to the Fermi level near the zone centre could also explain why it is difficult to image Si(001)–Bi(2 × n) with STM at positive bias (empty states). Since symmetric Bi dimers are known to be a basic building block of the Bi nanolines (Owen *et al* 2002b), we would expect the electronic structure of the nanoline to be semiconducting. This conjecture is confirmed by *ab initio* calculations of the nanoline electronic structure that will be presented in a future publication.

Acknowledgments

This research was supported by the Natural Sciences and Engineering Research Council of Canada. RHM was supported by CNPq and CAPES, Brazil.

References

Appelbaum J A, Baraff G A and Hamann D R 1976 *Phys. Rev.* B **14** 588
Asahi R, Mannstadt W and Freeman A J 2000 *Phys. Rev.* B **62** 2552
Bowler D R and Owen J H G 2002 *J. Phys.: Condens. Matter* **14** 6761

Chelikowsky J R, Wagener T J, Weaver J H and Jin A 1989 *Phys. Rev.* B **40** 9644
Corradini V, Gavioli L and Mariani C 1999 *Surf. Sci.* **430** 126
Cricenti A, Bernhoff H and Reihl B 1993 *Phys. Rev.* B **48** 10983
Cricenti A, Purdie D and Reihl B 1995 *Surf. Sci.* **331–333** 1033
Gay S C A, Jenkins S J and Srivastava G P 1998a *J. Phys.: Condens. Matter* **10** 7751
Gay S C A, Jenkins S J and Srivastava G P 1998b *Surf. Sci.* **402–404** 641
Hanada T and Kawai M 1990 *Vacuum* **41** 650
Hanada T and Kawai M 1991 *Surf. Sci.* **241** 137
Himpsel F J 1990a *Surf. Sci. Rep.* **12** 1
Himpsel F J 1990b *Phys. Scr.* T **31** 171
Johansson L S O and Reihl B 1992 *Surf. Sci.* **269–270** 810
Johnson P D and Hulbert S L 1990 *Rev. Sci. Instrum.* **61** 2277
Kentsch C, Kutschera M, Weinelt M, Fauster T and Rohlfing M 2002 *Phys. Rev.* B **65** 35323
Lipton-Duffin J A 2001 First results from a third generation kripes system *Master's Thesis* Queen's University
Lipton-Duffin J A, Mark A G and McLean A B 2002 *Rev. Sci. Instrum.* **73** 3149
Lipton-Duffin J A, Mark A G, Mullins G K, Contant G E and McLean A B 2004 *Rev. Sci. Instrum.* **75** 445
MacLeod J M, Moffat A, Miwa J A, Mark A G, Mullins G K, Dumont R H J, Contant G E and McLean A B 2003 *Rev. Sci. Instrum.* **74** 2429
McLean A B and Himpsel F J 1989 *Phys. Rev.* B **40** 8425
McLean A B, Ludeke R, Prietsch M, Heskett D, Tang D and Wong T M 1991 *Phys. Rev.* B **43** 7243
Miki K, Bowler D R, Owen J H G, Briggs G A D and Sakamoto K 1999a *Phys. Rev.* B **59** 14868
Miki K, Matsuhata H, Sakamoto K, Briggs G A D, Owen J H G and Bowler D R 1999b *Proc. Inst. Phys. Conf. Ser.* **164** 167
Naitoh M, Shimaya H, Nishigaki S, Oishi N and Shoji F 1997 *Surf. Sci.* **377–379** 899
Naitoh M, Shimaya H, Nishigaki S, Oishi N and Shoji F 1999 *Appl. Surf. Sci.* **142** 38
Naitoh M, Takei M, Nishigaki S, Oishi N and Shoji F 2000 *Japan. J. Appl. Phys.* **39** 2793
Naitoh M, Takei M, Nishigaki S, Oishi N and Shoji F 2001 *Surf. Sci.* **482–485** 1440
Northrup J E 1993 *Phys. Rev.* B **47** 10032
Ortega J E and Himpsel F J 1993 *Phys. Rev.* B **47** 2130
Owen J H G, Bowler D R and Miki K 2002a *Surf. Sci.* **499** L124
Owen J H G, Miki K and Bowler D R 2003 *Surf. Sci. Lett.* **527** L177
Owen J H G, Miki K, Koh H, Yeom H W and Bowler D R 2002b *Phys. Rev. Lett.* **88** 226104
Perfetti P and Reihl B 1989 *Phys. Scr.* T **25** 173
Park C, Bakhtizin R Z, Hashizume T and Sakurai T 1993 *Japan. J. Appl. Phys.* **32** L528
Park C, Bakhtizin R Z, Hashizume T and Sakurai T 1994 *J. Vac. Sci. Technol.* B **12** 2049
Reihl B, Magnusson K O, Nicholls J M, Perfetti P and Salvan F 1989 *NATO ASI Series on Metallization and Metal–Semiconductor Interfaces* (New York: Plenum)
Rohlfing M, Krüger P and Pollmann J 1995 *Phys. Rev.* B **52** 13753
Sakamoto K, Kyoya K, Miki K and Matsuhata H 1993 *Japan. J. Appl. Phys.* **32** L204
Srivastava G P 1999 *Theoretical Modelling of Semiconductor Surfaces* (Singapore: World Scientific)
Stoffel N G and Johnson P D 1984 *Nucl. Instrum. Methods* A **234** 230
Wolkow R A 1992 *Phys. Rev. Lett.* **68** 2636